ELSEVIER

Biophysical Chemistry 121 (2006) 171 – 176

Biophysical Chemistry

http://www.elsevier.com/locate/biophyschem

Interfacial properties of the M1 segment of the nicotinic acetylcholine receptor

Ernesto E. Ambroggio [a], Marcos A. Villarreal [a], Guillermo G. Montich [a], Dirk T.S. Rijkers [c], Maurits R.R. De Planque [b], Frances Separovic [b], Gerardo D. Fidelio [a,*]

[a] *CIQUIBIC-CONICET, Departamento de Química Biológica, Facultad de Ciencias Químicas, Haya de la Torre y Medina Allende, Ciudad Universitaria, Córdoba, Argentina, (CP X5000HUA)*

[b] *School of Chemistry, University of Melbourne, Melbourne VIC 3010, Australia*

[c] *Department of Medicinal Chemistry, Utrecht University, Sorbonnelaan 16, 3584 CA Utrecht, The Netherlands*

Received 7 October 2005; received in revised form 14 December 2005; accepted 15 December 2005
Available online 13 February 2006

Abstract

We have studied the thermodynamic, surface, and structural properties of αM1 transmembrane sequence of the nicotinic acetylcholine receptor (nAChR) by using Langmuir monolayer, FT-IR spectroscopy and molecular dynamics simulation techniques in membrane-mimicking environments. M1 spontaneously incorporates into a lipid-free air–water interface, showing a favourable adsorption free energy of −7.2 kcal/mol. A cross-sectional molecular area of 210 $Å^2$/molecule, a surface potential of 4.2 fV/molecule and a high stability of the film were deducted from pure M1 monolayers. FT-IR experiments and molecular dynamics simulations in membrane-mimicking environments (sodium-dodecyl-sulfate and CCl_4, respectively) indicate coexistence between helical and non-helical structures. Furthermore, mixed peptide–lipid monolayers and monolayer penetration experiments were performed in order to study the peptide–lipid interaction. Mixed with condensed lipids (dipalmitoyl-phosphocholine, and dipalmitoyl-phosphoglycerol), M1 shows immiscible/miscible behaviour at low/high peptide concentration, respectively. Conversely, a complete miscible peptide–lipid interface is observed with liquid-expanded lipids (palmitoyl-oleoyl-phosphocholine, and palmitoyl-oleoyl-phosphoglycerol). Peptide penetration experiments demonstrate that the M1 peptide preferentially interacts with zwitterionic phosphocholine interfaces.

Keywords: Peptide monolayer; Peptide–lipid interaction; Peptide–lipid mixed monolayers; Nicotinic acetylcholine receptor; Gibbs adsorption free energy; Molecular dynamics simulation; Peptide secondary structure; Distorted helix; Fourier-transform infrared spectroscopy; Transmembrane αM1 peptide

1. Introduction

The hydrophobic M1 peptide (H_2N-Ile-Met-Gln-Arg-Ile-Pro-Leu-Tyr-Phe-Val-Val-Asn-Val-Ile-Ile-Pro-Cys-Leu-Leu-Phe-Ser-Phe-Leu-Thr-Gly-Leu-Val-Phe-Tyr-Leu-Pro-Thr-Asp-Ser-Gly-COOH) corresponds to one of the α-subunit transmembrane segments of the best characterized members of the ligand-gated ion channels, the nicotinic acetylcholine receptor (nAChR) from *Torpedo californica* [1]. The receptor is composed of five subunits ($\alpha_2\beta\gamma\delta$) with homologous transmembrane domains, each consisting of four hydrophobic segments, M1–M4 (20–30 mers) [2]. Originally, all the four M–segments were proposed to be membrane-spanning α-helices by hydropathy profile analysis [3–5] but this remains as matter of debate. Méthot and Baenziger concluded from FT-IR measurements on the entire nAChR that the transmembrane domain is composed mainly of α-helices [6]. Also, as isolated peptides, M2, M3 and M4 seem to adopt a well-defined α-helical structure [7–10]. In contrast, the M1 segment seems to adopt a distorted helical conformation, exhibiting a bend, which is proposed to be due to the presence of proline residues in the M1 sequence [11–13].

Recently, Separovic and coworkers demonstrated that synthetic M1 peptide strongly interacts with model membranes and that the secondary structure of M1 incorporated in fluid-state phosphatidylcholine model membranes is not well defined near the central Pro residue. At this site, the peptide could be

* Corresponding author. Tel.: +54 351 4334168; fax: +54 351 4334174.
E-mail address: gfidelio@dqb.fcq.unc.edu.ar (G.D. Fidelio).

0301-4622/$ - see front matter © 2006 Elsevier B.V. All rights reserved.
doi:10.1016/j.bpc.2005.12.007

found with almost equal probability in a helical or a non-helical conformation, suggesting that the conserved Pro residue imparts conformational flexibility on M1 [14,15].

Here we report a thermodynamic and structural study of the transmembrane M1 sequence itself and of its interaction with lipids, by using the lipid monolayer technique, FT-IR spectroscopy and molecular dynamics (MD) simulations. Peptide penetration experiments into water–lipid interfaces indicate that the M1 peptide interacts preferentially with zwitterionic POPC monolayers, compared with anionic POPG monolayers. The monolayer data demonstrate that the M1 peptide has high surface activity, is not entirely helical in different membrane environments, and that its interaction with lipids depends on both the phase-physical state (condensed or expanded phase state) and the net charge of the lipids. FT-IR studies of M1 in SDS micelles indicate the presence of both helical and non-helical structural elements. Moreover, in MD simulations of the M1 sequence in a membrane-mimicking environment, the peptide adopts a kinked conformation.

2. Materials and methods

2.1. Chemicals

DPPC (1,2-dipalmitoyl-*sn*-glycero-3-phosphocholine), DPPG (1,2-dipalmitoyl-*sn*-glycero-3-[phospho-rac-(1-glycerol)]), POPC (1-palmitoyl-2-oleoyl-*sn*-glycero-3-phosphocholine) and POPG (1-palmitoyl-2-oleoyl-*sn*-glycero-3-[phospho-rac-(1-glycerol)]) were purchased from Avanti Polar Lipids Inc (Birmingham, AL) and were used without further purification.

The M1 peptide was synthesized using Fmoc chemistry as described earlier [14]. The peptide was purified by size exclusion chromatography on a Sephadex LH20 column with dichloromethane/methanol (1 : 1 v/v) as eluent. Peptide purity was analyzed by analytical HPLC on a Merck LiChroSpher CN column and determined to be 90% pure or higher. The peptide was characterized by mass spectrometry and a value of 3973.23 was found compared to the calculated average mass of [M+ H]+ 3973.85. The details are described in [14].

2.2. Monolayer studies

Monolayer experiments were performed at room temperature, (25 ± 2) °C. The subphase was 145 mM NaCl. Adsorption and penetration experiments were done by injecting the peptide from a dimethyl sulfoxide (DMSO) solution (0.12 mM peptide) into 18 ml of subphase contained in an 18 cm^2 trough. Lipids were dissolved in chloroform : methanol (67 : 33, v/v) solution. Pure peptide monolayers were formed by direct spreading from DMSO : chloroform : methanol (1 : 6 : 3, v/v) solution (0.19 mM) by using a microsyringe. For compression experiments the total surface area of the Teflon trough was 80 cm^2 and the volume of the subphase was 75 ml. The spreading solvent was allowed to evaporate for at least 5 min before compression was started, at a rate of 43 cm^2/min. Lower compression rates gave the same results. For lipid–peptide mixed monolayers, peptide and lipid were premixed at the desired proportion from their respective pure solutions, and then directly spread on the surface. The surface pressure (*Π*) (Wilhelmy method via platinized-Pt plate), the area enclosing the monolayer, and the surface potential (ΔV) (via milliVoltmeter with air-ionizing ^{241}Am plate and calomel electrode pair) were automatically measured (with the control unit Monofilmmeter with Film Lift, Mayer Feintechnique, Göttingen, Germany). The data were recorded continuously and simultaneously with a double channel X-YY recorder.

2.3. Transmission infra-red studies

FT-IR spectra of M1 (6.7 mg/ml) in a 15% SDS solution in ^2H_2O were recorded 12 h after sample preparation (to ensure a complete H/D exchange) on a Nicolet Nexus spectrometer, at room temperature in a CaF_2 cell with a 0.1 μm Teflon spacer, continuously purged with dry air to eliminate water vapour interference. 100 scans were signal-averaged at a resolution of 2 cm^{-1}. Before FT-IR measurements, M1 peptide was lyophilized several times from 10 mM HCl in order to eliminate traces of TFA. Spectra of peptide-free samples were subtracted from the spectra of the M1-containing samples, using OMNIC E.S.P. 5.1 software. Fourier self-deconvolution was performed and the values for the bandwidth and the enhancement for the deconvoluted spectra were 18 cm^{-1} and 2, respectively. The band fitting was performed as described by Nolan et al. [16].

2.4. Molecular dynamics simulation

A membrane-mimicking simulation box was constructed by stacking an equilibrated box of water, a box of carbon tetrachloride (CCl_4), and another box of water (Fig. 4). This membrane-mimicking box was equilibrated for 1 ns, and subsequently the M1 peptide, modelled as an ideal α-helix, was inserted in a transmembrane orientation. Water and CCl_4 molecules in contact with the peptide were removed. The final system was composed of one peptide, 160 mol of CCl_4 and 1400 mol of water. The dimension of the box was 34, 34, 70 Å in the *x*, *y*, *z* directions, with *z* being the axis normal to the interface. The CCl_4 layer had a thickness of 28 Å, a value close to the hydrophobic thickness of a POPC bilayer in the fluid state [17]. A second equilibration of 1 ns was performed, in which the peptide was subjected to position restraint forces on the backbone atoms. From this equilibrated structure, we removed the restraint forces on the peptide, and generated a production simulation of 24 ns in the NVT ensemble. The GROMOS G53a5 force field [18] was used for the peptide and the CCl_4 molecules. The water was modeled with the SPC potential. The dummy atom technique, together with the LINCS [19] constraint algorithm, allowed a time step of 4 fs. The non-bonded interactions were handled with the same techniques and parameters as used for the force field. Briefly, they include a reaction field for the electrostatics and a 1.4 nm cut-off distance for the van der Waals interaction. The temperature was maintained at 37 °C with the Berendsen thermostat [20], using a 0.2 ps time constant.

3. Results and discussion

3.1. Peptide adsorption at the air–water interface

The M1 peptide has a high surface activity. This property is deducted from the ability of M1 peptide to spontaneously adsorb into the air–water interface when it is injected in the subphase. The maximal equilibrium surface pressure reached by the peptide adsorption (Π_{eq}) was 27 mN/m, as it is shown in Fig. 1. The corresponding surface potential at this lateral pressure is 270 mV. From the adsorption experiments it is possible to know the thermodynamic tendency of an amphiphilic molecule partitioning into a lipid-free interface. The free energy of the adsorption process, ΔG_{ads}, can be calculated by using the Eq. (1):

$$\Delta G_{ads} = -RT\ln\frac{C_i}{C_s} \quad (1)$$

where C_i and C_s are the molar concentrations of the adsorbed molecules at the interface and subphase, respectively, T is the temperature (295 K) and R is the gas constant [21–24]. C_i can be estimated from the molecular area obtained from the compression isotherm of pure peptide monolayers (see below; Fig. 2). If the M1 peptide is assumed to be perpendicular to the interface we consider a thickness equivalent to the peptide length of about 52.5 Å (1.5 Å per residue for an α-helical structure, see [21]). With these assumptions, the M1 peptide has a free energy of −7.2 kcal/mol for the adsorption process into the free lipid air–water interface and as is similar for other membrane-interacting peptides such as Australian tree frog antimicrobial peptides and melittin [21,25].

3.2. Pure peptide spread monolayers

Pressure–Area (Π–A) isotherms of M1 peptide monolayers reveal that the peptide forms insoluble films at the air–water interface showing high lateral stability comparable to fluid-state lipids, like pure POPC monolayers (Fig. 2). The M1 film has a high collapse pressure (Π_c) of 41 mN/m. The deduced peptide molecular area obtained from Π–A isotherms at this

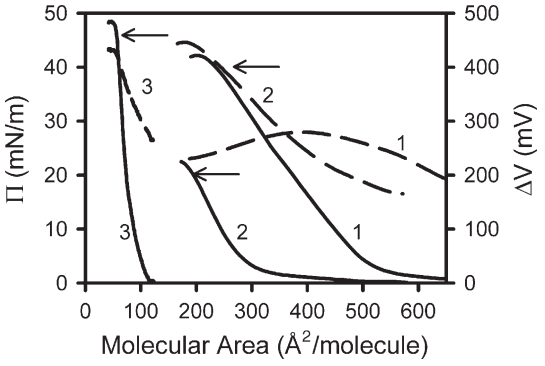

Fig. 2. Surface behaviour of pure M1 peptide (1), melittin (2) and POPC (3) at the air–water interface. Π–Area (solid line) and ΔV–Area (dashed line) isotherms. Arrows indicate the collapse pressure (Π_c) of monolayers. Subphase: 145 mM NaCl.

maximal molecular packing (at the Π_c) is 210 Å^2/molecule. The surface potential at this point is 200 mV. These parameters are somewhat in between the values observed for monolayers formed by α-helical or β-sheet peptides [21,25]. Monolayers of peptides in an α-helical conformation show a low collapse pressure, a high surface potential, and molecular areas in the range of 150–190 Å^2/mol as it is illustrated in Fig. 2 for the well-known α-helical peptide, melittin [21,26,27]. On the other hand, a film composed of an extended β-sheet structured peptide has high lateral stability (high Π_c), low surface potential, and molecular areas of about 70 Å^2 [25,28]. In our case, M1 peptide seems to adopt a global helical configuration at the Π_c but the other parameters are in agreement with non-helical structures. The molecular area obtained for the M1 peptide is higher than expected for a peptide that adopts an "ideal" α-helix (180 Å^2/molecule, see [21]). This may well be possible if the peptide adopts a distorted helical conformation or mixed structures at the interface [29].

3.3. Infra-red spectroscopy

A direct structural analysis of M1 peptide in a membrane environment was performed using FT-IR spectroscopy. Fig. 3

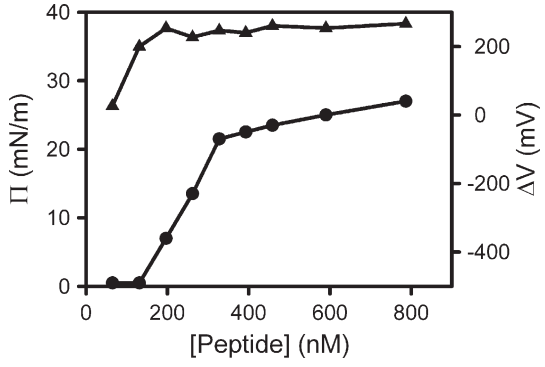

Fig. 1. Adsorption of M1 peptide into lipid-free air–water interface. Surface lateral pressure (Π, circle) and surface potential (ΔV, triangle) dependence with peptide concentration injected into 145 mM NaCl subphase.

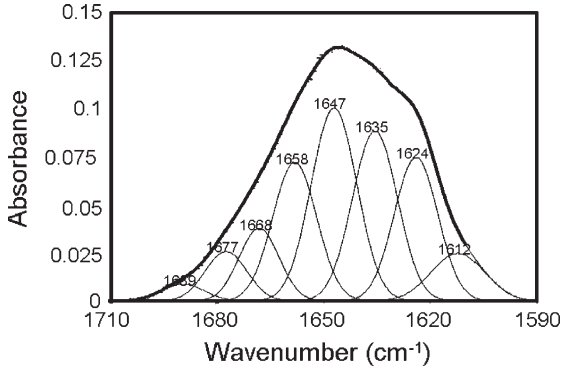

Fig. 3. FT-IR absorbance spectrum of M1 peptide in 15% SDS solution. Gaussian curves are the spectral components obtained by curve fitting from the deconvoluted spectrum. The peptide concentration is 6.7 mg/ml.

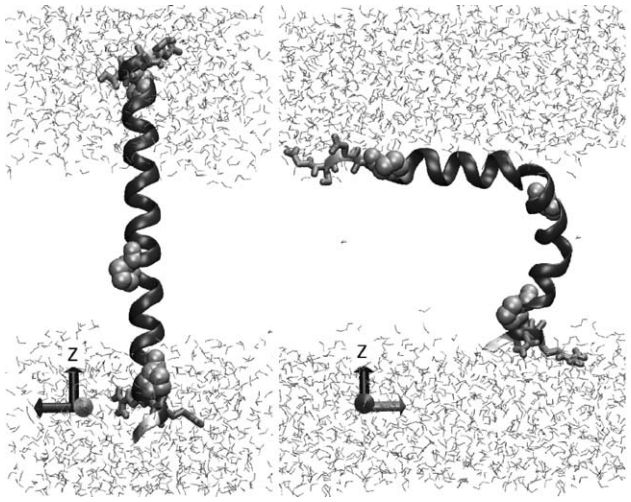

Fig. 4. Initial (left) and final (right) structures from the simulation of the M1 peptide in a CCl_4 membrane-mimicking environment. The backbone of the peptide is shown as a ribbon, the proline residues are in space-filling representation. The hydrophilic residues anchoring the peptide to the water face, Gln-3 and Arg-4 (upper layer) and Thr-34, Asp-35, Ser-36 and Gly-37 (lower layer) are pictured as licorice. For visualization proposes, only water molecules are shown, while CCl_4 molecules were removed. In both panels, the N-terminal side of the peptide is located at the upper layer.

shows the FT-IR transmission spectrum of M1 in D_2O containing 15% SDS. The main band at 1647 cm^{-1} (amide I region) is in agreement with a peptide adopting a helical structure [30]. In addition, non-helical structural elements are also present as indicated by the bands at 1624, 1635, 1658 and 1677 cm^{-1}, which correspond to extended sheets and turns [30]. The bands at 1624 and 1635 cm^{-1} can be assigned to a β-sheet conformation. On the other hand, the bands between 1656 and 1680 cm^{-1} are in agreement with a distortion of the helical conformation [30,31]. This data indicates that the M1 sequence does not adopt a simple conformation in an SDS environment, in accordance with previous reports [12,15]. SDS micelles were used as a membrane-mimicking environment, although due to high surface curvature and dynamically large fluctuations, do not accurately represent the membrane bilayer. Nevertheless, our FTIR results are in agreement with CD and NMR structural studies of M1 in DMPC bilayers, which also show conformational heterogeneity of the peptide [15].

3.4. Computer simulations

The peptide conformation adopted in a membrane environment also was investigated by MD simulations. The simulation was initiated with the peptide in a transmembrane orientation with an ideal α-helical conformation in an environment with similar dielectric constant to a membrane, as used in other recent simulations [32] (see Fig. 4). After 0.1 ns the helix began to bend at the Pro-16 residue and after 10 ns the peptide adopted the conformation depicted in Fig. 4. This conformation was maintained for the remaining 14 ns of the simulation. The sequence of M1 is highly hydrophobic, with 25 apolar residues

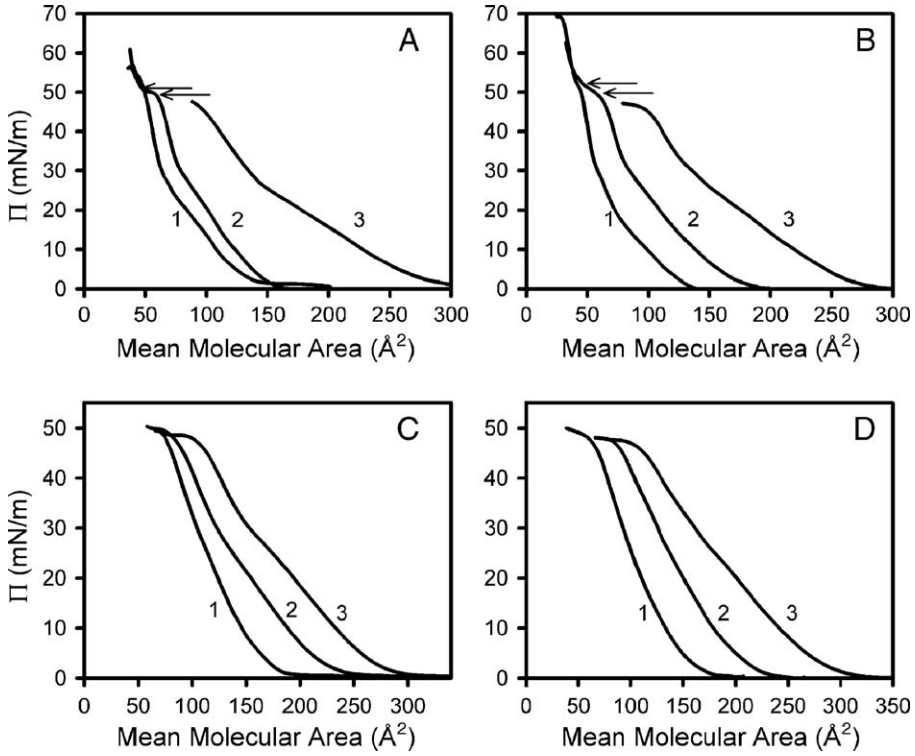

Fig. 5. *Π*–Area compression isotherms of peptide–lipid mixed monolayers. (A) M1-DPPC, (B) M1-DPPG, (C) M1-POPC, and (D) M1-POPG peptide–lipid mixed monolayers with peptide to lipid area ratios of 25 : 75 (curve 1; A and B: 0.06 : 0.94; C: 0.09 : 0.91; D: 0.08 : 0.92 peptide : lipid mole ratio), 50 : 50 (curve 2; A and B: 0.15 : 0.85; C and D: 0.22 : 0.78 peptide : lipid mole ratio), 75 : 25 (curve 3; A and B: 0.39 : 0.61; C: 0.47 : 0.53; D : 0.45 : 0.55 peptide : lipid mole ratio). Arrows indicate the collapsing point of the peptide-enriched phase. Subphase: 145 mM NaCl.

out of 35. The hydration of polar residues located at the extremes of the sequence prevents the M1 peptide from being located entirely in the organic phase. The residues that help to anchor the peptide in the final orientation are Gln-3 and Arg-4 at the N-terminus, together with Thr-34, Asp-35, Ser-36 and Gly-37 at the C-terminus. The kinked conformation obtained in the simulation is consistent with the monolayer results, which suggested a deformed α-helix, and also with the FT-IR data, which indicated the coexistence of helical and non-helical conformations.

3.5. Lipid–peptide monolayers

The monolayer technique is a powerful tool to study lipid–peptide interactions [16,21]. This unique technique allows working with a known lipid–peptide ratio at the interface. In our experiments we used peptide mole fractions equivalent to 25%, 50% and 75% of area covered by the peptide in the peptide–lipid mixed interface (see legend to Fig. 5). The peptide mole fraction is lower than that of the lipid due to the dissimilar individual molecular areas of the lipid compared with that obtained for pure M1 peptide in monolayers.

The studies of mixed monolayers showed a dual behaviour for the lipid–peptide interaction. Peptide–lipid monolayers composed of M1 mixed with either zwitterionic DPPC (Fig. 5A) or negatively charged DPPG lipids (Fig. 5B) were analyzed. Both lipids are in a liquid condensed (LC) phase state at lateral pressures higher than 10 mN/m. From Fig. 5A and B, two collapse pressures were observed in the isotherm at low peptide content. The low collapse pressure (arrows) corresponds to the collapse pressure of a peptide-enriched phase. The high collapsing point is the collapse of the lipid-enriched phase. The presence of this two collapse pressures in the compression isotherm means lateral immiscibility [33]. On the other hand, only one collapse pressure is observed at the highest peptide proportion used, indicating that in this condition the peptide and the lipid are miscible [32]. Alternatively, monolayers of M1 mixed with lipids in a liquid-expanded (LE) phase state were also studied. The lipids in a LE phase state used were the zwitterionic POPC (Fig. 5C) and the anionic POPG (Fig. 5D). For both mixed interfaces a miscible behaviour was observed. This can be concluded because only one collapse pressure is observed and this value falls in between the collapse pressures of the pure components [21,29,33]. In both cases (immiscibility or miscibility), no significant lipid–peptide interaction, in repulsive or attractive terms, was observed. This is concluded because the experimental mean molecular areas of the mixed films showed no significant deviations from the ideal behaviour (see, [24]). These findings highlight the influence of the physical state of the lipids on peptide–lipid miscibility.

3.6. Peptide penetration

Penetration experiments measure the ability of a peptide to be incorporated into a pre-organized lipid interface [21,24,26,33]. Fig. 6 shows the maximum change in surface pressure acquired by the interface as a consequence of peptide interaction (i.e., peptide insertion; $\Delta\Pi_{max}$) in function of the initial pressure of the lipid monolayer (density of the lipid array; Π_{Lipid}). As it can be seen in Fig. 6 M1 strongly interacts with POPC and POPG (both lipids that were miscible with M1 in mixed monolayers). From the penetration data, a cut-off surface pressure point was calculated which means the highest lateral packing in which no further penetration is observed. This was obtained by extrapolating the linear dependence of $\Delta\Pi_{max}$ with Π_{Lipid} (Fig. 6). Evidently, M1 penetrates easier into POPC monolayers than into POPG monolayers. The penetration of M1 into POPC films has a cut-off surface pressure that is 10 mN/m higher than in the case of POPG monolayers, indicating a higher spontaneous interaction for the zwitterionic lipid.

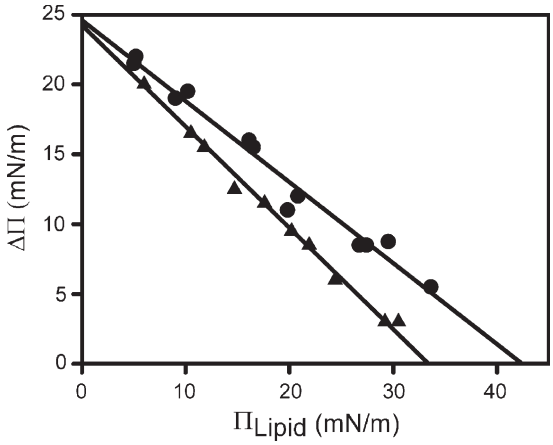

Fig. 6. Penetration of M1 peptide into POPC (circle) and POPG (triangle) monolayers. Maximum increase in surface pressure ($\Delta\Pi_{max}$) as a function of Π_{Lipid} of POPC (circle) and POPG (triangle) upon injection of M1 peptide at a concentration of 655 nM. Subphase 145 mM NaCl.

4. Conclusions

In the present biophysical study we demonstrate that the M1 transmembrane segment of the nAChR has a high spontaneous surface activity, with a free energy of adsorption into a air–water interface of $\Delta G_{ads} = -7.2$ kcal/mol. Pure peptide monolayer data indicated that the molecular area of M1 correlates with a possible mixture of conformations at the air–water interface [29]. Coexisting helical and non-helical structural elements in M1 were evident by FT-IR measurements and molecular dynamics simulations. Furthermore, mixed peptide–lipid monolayer studies showed that the M1 peptide is completely miscible with lipids in the liquid expanded phase state and, this together with the peptide penetration results, led us to conclude that the M1 peptide behaves as an "ideal partner" with the more liquid zwitterionic PC. We speculate that the conserved central Pro residue confers a conformational flexibility on the M1 segment, which distinguishes M1 from the other transmembrane segments, M2, M3 and M4. Such a conformational flexibility may play a role in the regulation of the nAChR, which has been shown to depend, among other factors, upon the physical state of the membrane [34].

Acknowledgment

This work was supported by grants from CONICET, FONCYT (PICT 0609228), SECYT-UNC, and Agencia Córdoba Ciencia. G. D. F. and G. G. M. are members of the Career of Investigator. E. E. A. and M. A. V. are fellows from CONICET. M. R. R. de P. was supported by fellowship S81-683 of The Netherlands Organization for Scientific Research (NWO).

References

[1] A. Karlin, Emerging structure of the nicotinic acetylcholine receptors, Nat. Rev. Neurosci. 3 (2002) 102–114.
[2] M.A. Raftery, M.W. Hunkapiller, C.D. Stader, L.E. Hood, Acetylcholine receptor: complex of homologous subunits, Science 208 (1980) 1454–1456.
[3] T. Claudio, M. Ballivet, J. Patrick, S. Heinemann, Nucleotide and deduced amino acid sequences of *Torpedo californica* acetylcholine receptor gamma subunit, Proc. Natl. Acad. Sci. U. S. A. 80 (1983) 1111–1115.
[4] M. Noda, H. Takahashi, T. Tanabe, M. Toyosato, Y. Furutani, T. Hirose, M. Asai, S. Inayama, T. Miyata, S. Numa, Primary structure of alpha-subunit precursor of *Torpedo californica* acetylcholine receptor deduced from cDNA sequence, Nature 229 (1982) 793–797.
[5] M. Noda, H. Takahashi, T. Tanabe, M. Toyosato, S. Kikyotani, T. Hirose, M. Asai, H. Takashima, S. Inayama, T. Miyata, S. Numa, Primary structures of beta- and delta-subunit precursors of *Torpedo californica* acetylcholine receptor deduced from cDNA sequences, Nature 301 (1983) 251–255.
[6] N. Méthot, J.E. Baenziger, Secondary structure of the exchange-resistant core from the nicotinic acetylcholine receptor probed directly by infrared spectroscopy and hydrogen/deuterium exchange, Biochemistry 37 (1998) 14815–14822.
[7] S.J. Opella, F.M. Marassi, J.J. Gesell, A.P. Valente, Y. Kim, M. Oblatt-Montal, M. Montal, Structures of the M2 channel-lining segments from nicotinic acetylcholine and NMDA receptors by NMR spectroscopy, Nat. Struct. Biol. 6 (1999) 374–379.
[8] P.T.F. Williamson, B.B. Bonev, F.J. Barrantes, A. Watts, Structural characterization of the M4 transmembrane domain of the acetylcholine receptor: an NMR study, Biophys. J. 78 (2000) 147.
[9] V.S. Pashkov, I.V. Maslennikov, L.D. Tchikin, R.G. Efremov, V.T. Ivanov, A.S. Arseniev, Spatial structure of the M2 transmembrane segment of the nicotinic acetylcholine receptor alpha-subunit, FEBS Lett. 457 (1999) 117–121.
[10] A.A. Lugovskoy, I.V. Maslennikov, Y.N. Utkin, V.I. Tsetlin, J.B. Cohen, A.S. Arseniev, Spatial structure of the M3 transmembrane segment of the nicotinic acetylcholine receptor alpha subunit, Eur. J. Biochem. 255 (1998) 455–461.
[11] F.J. Barrantes, S.S. Antollini, M.P. Blanton, M. Prieto, Topography of nicotinic acetylcholine receptor membrane-embedded domains, J. Biol. Chem. 275 (2000) 37333–37339.
[12] J. Corbin, N. Méthot, H.H. Wang, J.E. Baenziger, M.P. Blanton, Secondary structure analysis of individual transmembrane segments of the nicotinic acetylcholine receptor by circular dichroism and Fourier transform infrared spectroscopy, J. Biol. Chem. 273 (1998) 771–777.
[13] A. Miyazawa, Y. Fujiyoshi, N. Unwin, Structure and gating mechanism of the acetylcholine receptor pore, Nature 423 (2003) 949–955.
[14] M.R. de Planque, D.T. Rijkers, R.M. Liskamp, F. Separovic, The αM1 transmembrane segment of the nicotinic acetylcholine receptor interacts strongly with model membranes, Magn. Reson. Chem. 42 (2004) 148–154.
[15] M.R. de Planque, D.T. Rijkers, J.I. Fletcher, R.M. Liskamp, F. Separovic, The αM1 segment of the nicotinic acetylcholine receptor exhibits conformational flexibility in a membrane environment, Biochim. Biophys. Acta 1665 (2004) 40–47.
[16] V. Nolan, M. Perduca, H.L. Monaco, B. Maggio, G.G. Montich, Interactions of chicken liver basic fatty acid-binding protein with lipid membranes, Biochim. Biophys. Acta 1611 (2003) 98–106.
[17] B.A. Lewis, D.M. Engelman, Lipid bilayer thickness varies linearly with acyl chain length in fluid phosphatidylcholine vesicles, J. Mol. Biol. 166 (1983) 211–217.
[18] C. Oostenbrink, A. Villa, A.E. Mark, W.F. van Gunsteren, A biomolecular force field based on the free enthalpy of hydration and solvation: the GROMOS force-field parameter sets 53A5 and 53A6, J. Comput. Chem. 25 (2004) 1656–1676.
[19] B. Hess, H. Bekker, H.J.C. Berendsen, J.G.E.M. Fraaije, LINCS: a linear constraint solver for molecular simulations, J. Comput. Chem. 18 (1997) 1463–1472.
[20] H.J.C. Berendsen, J.P.M. Postma, W.F. van Gunsteren, A. DiNola, J.R. Haak, Molecular dynamics with coupling to an external bath, J. Chem. Phys. 81 (1984) 3684–3690.
[21] E.E. Ambroggio, F. Separovic, J. Bowie, G.D. Fidelio, Surface behaviour and peptide-lipid interactions of the antibiotic peptides, Maculatin and Citropin, Biochim. Biophys. Acta 1664 (2004) 31–37.
[22] G. Gonzalez, F. MacRitchie, Equilibrium adsorption of proteins, J. Colloid Interface Sci. 32 (1970) 55–61.
[23] F. MacRitchie, Proteins at interfaces, Adv. Protein Chem. 32 (1978) 283–326.
[24] K.S. Birdi, Kinetics of adsorption and desorption, Lipid and Biopolymer Monolayers at Liquid Interfaces, Plenum Press, New York, 1989.
[25] R. Maget-Dana, D. Lelièvre, A. Brack, Surface active properties of amphiphilic sequential isopeptides: comparison between alpha-helical and beta-sheet conformations, Biopolymers 49 (1999) 415–423.
[26] R. Maget-Dana, The monolayer technique: a potent tool for studying the interfacial properties of antimicrobial and membrane-lytic peptides and their interactions with lipid membranes, Biochim. Biophys. Acta 1462 (1999) 109–140.
[27] G.D. Fidelio, B. Maggio, F.A. Cumar, Interaction of melittin with glycosphingolipids and phospholipids in mixed monolayers at different temperatures. Effect of the lipid physical state, Biochim. Biophys. Acta 862 (1986) 49–56.
[28] G.D. Fidelio, B.M. Austen, D. Chapman, J.A. Lucy, Properties of signal-sequence peptides at an air–water interface, Biochem. J. 238 (1986) 301–304.
[29] E.E. Ambroggio, D.H. Kim, F. Separovic, C.J. Barrow, K.J. Barnham, L. A. Bagatolli, G.D. Fidelio, Surface behavior and lipid interaction of Alzheimer beta-amyloid peptide 1–42: a membrane-disrupting peptide, Biophys. J. 88 (2005) 2706–2713.
[30] J.L. Arrondo, A. Muga, J. Castresana, F.M. Goñi, Quantitative studies of the structure of proteins in solution by Fourier-transform infrared spectroscopy, Prog. Biophys. Mol. Biol. 59 (1993) 23–56.
[31] D. Avrahami, Z. Oren, Y. Shai, Effect of multiple aliphatic amino acids substitutions on the structure, function, and mode of action of diastereomeric membrane active peptides, Biochemistry 40 (2001) 12591–12603.
[32] A. Hung, K. Tai, M.S. Sansom, Molecular dynamics simulation of the M2 helices within the nicotinic acetylcholine receptor transmembrane domain: structure and collective motions, Biophys. J. 88 (2005) 3321–3333.
[33] G.L. Gaines, Insoluble Monolayers at Liquid–Gas Interfaces, Prigogine editor, Interscience, New York, 1966.
[34] J.E. Baenziger, M.L. Morris, T.E. Darsaut, S.E. Ryan, Effect of membrane lipid composition on the conformational equilibria of the nicotinic acetylcholine receptor, J. Biol. Chem. 275 (2000) 777–784.